

# Novel Characteristics of the Biological Properties of the Yeast *Saccharomyces cerevisiae* Eukaryotic Initiation Factor 2A\*

Received for publication, December 6, 2004, and in revised form, February 1, 2005  
Published, JBC Papers in Press, February 16, 2005, DOI 10.1074/jbc.M413728200

Anton A. Komar<sup>‡</sup>, Stephane R. Gross<sup>§</sup>, Diane Barth-Baus<sup>‡¶</sup>, Ryan Strachan<sup>‡</sup>, Jack O. Hensold<sup>¶</sup>,  
Terri Goss Kinzy<sup>§</sup>, and William C. Merrick<sup>‡||</sup>

From the <sup>‡</sup>Department of Biochemistry, Case Western Reserve University School of Medicine, Cleveland, Ohio 44106, the <sup>§</sup>Department of Molecular Genetics, Microbiology, and Immunology, University of Medicine and Dentistry of New Jersey Robert Wood Johnson Medical School, Piscataway, New Jersey 08854, and the <sup>¶</sup>Veterans Affairs Medical Center and Department of Medicine, Case Western Reserve University School of Medicine, Cleveland, Ohio 44106

Eukaryotic initiation factor 2A (eIF2A) has been shown to direct binding of the initiator methionyl-tRNA (Met-tRNA<sub>i</sub>) to 40 S ribosomal subunits in a codon-dependent manner, in contrast to eIF2, which requires GTP but not the AUG codon to bind initiator tRNA to 40 S subunits. We show here that yeast eIF2A genetically interacts with initiation factor eIF4E, suggesting that both proteins function in the same pathway. The double *eIF2A/eIF4E-ts* mutant strain displays a severe slow growth phenotype, which correlated with the accumulation of 85% of the double mutant cells arrested at the G<sub>2</sub>/M border. These cells also exhibited a disorganized actin cytoskeleton and elevated actin levels, suggesting that eIF2A might be involved in controlling the expression of genes involved in morphogenic processes. Further insights into eIF2A function were gained from the studies of eIF2A distribution in ribosomal fractions obtained from either an *eIF5BΔ* (*fun12Δ*) strain or a *eIF3b-ts* (*prt1-1*) strain. It was found that the binding of eIF2A to 40 and 80 S ribosomes was not impaired in either strain. We also found that eIF2A functions as a suppressor of Ure2p internal ribosome entry site-mediated translation in yeast cells. The regulation of expression from the *URE2* internal ribosome entry site appears to be through the levels of eIF2A protein, which has been found to be inherently unstable with a half-life of ~17 min. It was hypothesized that this instability allows for translational control through the level of eIF2A protein in yeast cells.

Initiation of protein synthesis in eukaryotes is a complex process requiring numerous accessory proteins called initiation factors. At least 12 different initiation factors have been identified, comprising over 30 polypeptide chains (1). The function of many of these factors have been established in detail (1, 2); however, the precise role of some of them, their mechanism of action, and the particular step in the initiation process at which these factors function still remains obscure. It should be noted that recent studies have pointed to the key role of translational

control (which is mainly exerted at the initiation step of protein synthesis) in regulating gene expression during development, differentiation, cell cycle progression, cell growth, apoptosis, and stress (3–5). Studies of the responses of a large variety of cell systems to different physiological stimuli have shown that protein synthesis can be modulated by both changes in the state of phosphorylation of initiation factors and changes in the levels of these factors in the cell. These effects allow rapid modification of the overall rate of translation as well as post-transcriptional regulation of gene expression due to changes in the relative selection of different mRNA species utilizing different mechanisms of translation initiation. In view of these observations, it is of importance to establish the molecular mechanisms by which changes in the levels or activities of various initiation factors could affect cell fate.

Eukaryotic initiation factor 2A (eIF2A)<sup>1</sup> is a 65-kDa protein that was first identified in the early 1970s on the basis of its stimulation of initiator methionyl-tRNA (Met-tRNA<sub>i</sub>) binding to 40 S ribosomal subunits, its participation in methionyl puromycin synthesis, and its ability to stimulate poly(U)-directed polyphenylalanine synthesis at low [Mg<sup>2+</sup>]. eIF2A was initially believed to be the functional homologue of prokaryotic IF2, since IF2 catalyzes biochemically similar reactions (6, 7). Subsequent identification of a multisubunit factor eIF2 (8–10) showed that this factor and not eIF2A is primarily responsible for the delivery of Met-tRNA<sub>i</sub> to 40 S subunits in eukaryotes. Whereas both eIF2 and eIF2A function similarly in model assays, the order of events differs between the two (Fig. 1). eIF2A binds Met-tRNA<sub>i</sub> to 40 S subunits in a codon-dependent manner, whereas eIF2 binds Met-tRNA<sub>i</sub> to 40 S subunits in a GTP-dependent manner (7, 11–13). Recently, the yeast homologue of mammalian eIF2A was identified, and yeast strains were obtained that lacked the gene for eIF2A (14). The *eIF2AΔ* strains were viable and showed no apparent phenotype (although this strain sporulated with about one-third the efficiency of the wild type (14)), suggesting that the eIF2A does not function in major (key) steps in the initiation process but, perhaps, could act at some late steps or be involved in minor alternative initiation events such as reinitiation, internal initiation, or non-AUG initiation. Of these alternatives, it does not appear that eIF2A influences reinitiation, at least as tested using the *GCN4* reporter system in yeast cells (14). Genetic interaction of the eIF2A and eIF5B was also observed, suggest-

\* This work was supported by NIGMS, National Institutes of Health (NIH), Grants GM26796 and GM68079 (to W. C. M.), NIDDK, NIH, Grant DK43414 (to J. O. H.), and NIH Grant GM62789 (to T. G. K. and S. R. G.). The costs of publication of this article were defrayed in part by the payment of page charges. This article must therefore be hereby marked "advertisement" in accordance with 18 U.S.C. Section 1734 solely to indicate this fact.

|| To whom correspondence should be addressed: Dept. of Biochemistry, Case Western Reserve University School of Medicine, Cleveland, OH 44106. Tel.: 216-368-3578; Fax: 216-368-3419; E-mail: wcm2@cwru.edu.

<sup>1</sup> The abbreviations used are: eIF2A, -3b, and -5B, eukaryotic initiation factor 2A, 3b, and 5B, respectively; HA, hemagglutinin; PBS, phosphate-buffered saline; WT, wild type; ts, temperature-sensitive; Tricine, N-[2-hydroxy-1,1-bis(hydroxymethyl)ethyl]glycine; IRES, internal ribosome entry site.

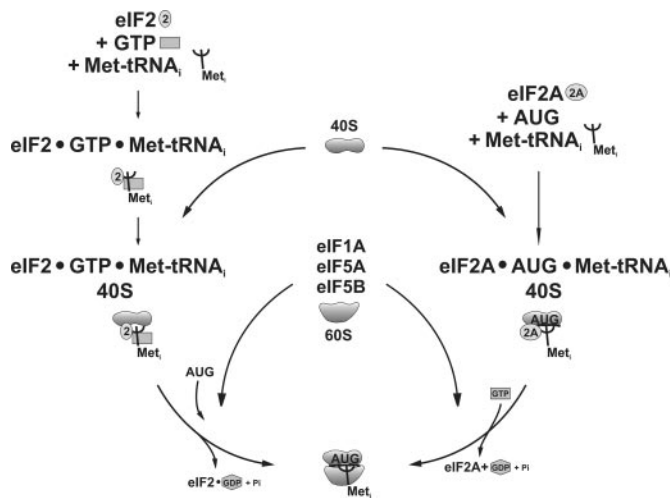


FIG. 1. Two pathways for the formation of model 80 S initiation complexes (adapted from Ref. 1 with the use of current nomenclature).

ing that both proteins function in the same pathway (14).

In this paper, we have further characterized the yeast *eIF2A* using both genetic and biochemical approaches. We show here that *eIF2A* genetically interacts with *eIF4E*, suggesting that both proteins function in the same pathway. The double *eIF2A/eIF4E-ts* mutant strain displayed a severe slow growth phenotype. This synthetic slow growth correlated with the accumulation of the double mutant cells arrested at the  $G_2/M$  border. Furthermore, disruption of the *eIF2A* gene in the *eIF4E-ts* strain 4-2 caused a strong disorganization of the actin cytoskeleton and accumulation of actin protein at elevated levels. We also show that *eIF2A* acts as a suppressor of the internal ribosome entry site (IRES) element found in the *URE2* mRNA. Analysis of *eIF2A* distribution in ribosomal fractions of various yeast mutants suggests that this inhibition occurs at the level of 40 S/80 S ribosomes. We also found that *eIF2A* is an inherently unstable protein with a half-life of ~17 min. We hypothesize that this instability allows for translational control through the level of *eIF2A* protein in yeast cells.

#### MATERIALS AND METHODS

**Yeast Strains and Growth Methods**—Yeast strains used in this study are listed in Table I. Wild-type BY4741 (*Mata, his3-1, leu2-0, met15-0, ura3-0*) and isogenic *eIF2AΔ* (*Mata, his3-1, leu2-0, met15-0, ura3-0, ygr054w::KanMX*) strains have been described previously (14) and were used in *lacZ* expression experiments. The disruption of the *eIF2A* gene in the *eIF2AΔ* strain (open reading frame YGR054W) was verified by PCR (with 5'-GTACTACAACAACAGTCAGGTTCAATAACACC-3' as the upstream and 5'-CACAGTTGTATGGATACATCAGTTTCTTCTAG-3' as the downstream primer). Strains H2879 (*MATa, leu2-3, leu2-112, ura3-52, PRT1*), H1676 (*MATa, leu2-3, leu2-112, ura3-52, prt1-1*), *GIM3Δ* (*Mata, his3-1, leu2-0, met15-0, ura3-0, gim3::KanMX*), *GIM5Δ* (*Mata, his3-1, leu2-0, met15-0, ura3-0, gim5::KanMX*) and *PAC10Δ* (*Mata, his3-1, leu2-0, met15-0, ura3-0, pac10::KanMX*) were kindly provided by Dr. Thomas Dever (National Institutes of Health). *eIF5BΔ* (*Mata, his3-1, leu2-0, met15-0, ura3-0, fun12::KanMX*) strain has been obtained from Research Genetics. The *eIF4E-ts* strain 4-2 (*MATa, ade2-1, leu2-3,112, his3-11,15, trp1-1, ura3, cdc33::LEU2 <cdc33-4-2; TRP1, ARSCEN>*) has also been previously described (15, 16). The *eIF4E-ts* strain 4-2/2A (*MATa, ade2-1, leu2-3,112, his3-11,15, trp1-1, ura3, ygr054w::KanMX, cdc33::LEU2 <cdc33-4-2; TRP1, ARSCEN>*) was obtained as follows. Genomic DNA from *eIF2AΔ* (*Mata, his3-1, leu2-0, met15-0, ura3-0, ygr054w::KanMX*) strain was amplified by PCR using 5'-CTTAGTGTTGATTGAGACGTGTTGTG-3' as an upstream and 5'-GGCGTAATTCTCTGGGAAACAG-3' as a downstream primer, and the PCR fragment was further used for transformation of the *eIF4E-ts* strain 4-2. Transformants, which were able to grow on medium containing G418 sulfate and showed a *ts*-phenotype, were further checked for homologous gene recombination by PCR.

Yeast cultures were grown as indicated using either synthetic me-

dium containing 0.67% Difco yeast nitrogen base, 1% ammonium sulfate, 2% glucose (or galactose) and supplemented with the appropriate amino acids or complete (YEED) medium (17). Transformation was performed using the lithium acetate method (18). For the polysome expression analysis of HA-tagged *eIF2A*, yeast were grown in complete medium with 2% galactose.

**Plasmids**—The pTB328\_y\_2A shuttle vector bearing yeast *eIF2A* (fused to an HA epitope) under control of the GAL promoter has been previously described (14). The YCplac111 (CEN, *LEU2*) vector bearing yeast *eIF2A* under its own promoter was produced by BamHI-PstI subcloning of the PCR-amplified (3339 bp) yeast genomic DNA fragment (with 5'-AACGCGGATCCCTATTATCTATGAATATAAACTGTCTATCTTTCC-3' as the upstream and 5'-AAAACGCGCAGCCATGGTGTGCAATAACTGCGAAGGTAGCACCGC-3' as the downstream primer) into the YCplac111 vector. This fragment contains 843 bp upstream of the *eIF2A* AUG start codon. The pRS316\_y\_2A (CEN, *URA3*) plasmid was constructed as follows. Yeast *eIF2A* genomic DNA fragment (3809 bp) was PCR-amplified with 5'-TTGGTTCAAATTATTGGCTGTAGG-3' as an upstream primer and 5'-TTGTATGGATGGATCCGTTTCTTCTAGTTTATTC-3' as downstream digested with KpnI and XhoI and cloned into KpnI-SalI-digested pRS316 vector. The pTB328\_h\_2A vector bearing the cDNA copy of human *eIF2A* under control of GAL promoter was produced as follows. cDNA encoding human *eIF2A* (I.M.A.G.E. Consortium Clone ID 3688407) was amplified by PCR (with 5'-AAACGCGGATCCATGGCGCCGCCACGCC-3' as the upstream and 5'-AAAACGCGCAGGTCTTTATTCATTACATGGTATATATCAC-3' as the downstream primer), digested with BamHI and PstI, and cloned into pTB328 (CEN, *LEU2*, *GAL1* promoter, HA tag) vector. The p281 plasmid containing *lacZ* under GAL promoter has been described previously (19). The pDAD2-*eIF4E*(HA tag) vector containing HA-tagged yeast *eIF4E* under the control of GAL promoter (*URA3* as an auxotrophic marker) was kindly provided by Dr. Nahum Sonenberg (McGill University). The p281-4-*URE2* and p281-4-*URE2\_CTT* vectors have also been previously described (20).

**Northern Blot Analysis**—Northern blotting was performed generally as described (21) with slight modifications following the general procedures described previously (20). For detection of *Ure2\_lacZ* mRNAs, the PCR-amplified 3-kb *lacZ* fragment (with 5'-CGCCTTGACGACATCC-3' as the upstream and 5'-GGTAGCGACCGGCGC-3' as the downstream primer) was random prime-labeled using the Ambion Random Primed Strip Able DNA probe synthesis and removal kit. RNA electrophoresis was accomplished using the Glyoxal-based system (Ambion). Ambion RNA Millennium Markers™ were used as molecular size standards. Yeast total RNA was prepared using the RNAqueous™ kit from Ambion. The 5'-end <sup>32</sup>P-labeled anti-HA primers (5'-GCCCCGATAGTCAGBAAACATCGTATGGGTA-3' for HA-*eIF2A* and 5'-AGAAGCGTAGTCTGGCAGTCGATGGGTA-3' for HA-*eIF4E*) were used to probe for *eIF2A* and *eIF4E* mRNAs expressed from the GAL promoter. Note that the nucleotide (but not the amino acid) sequence of HA tag attached to *eIF2A* and *eIF4E* open reading frames differs slightly, and this is why two different primers were used.

**Fractionation of Ribosomes**—Fractionation of ribosomes was performed essentially as described before (14). All procedures were performed at 4 °C except where indicated. Yeast cells from 50 ml of log phase culture were pelleted, treated for 1 min with 10 μg/ml cycloheximide (Calbiochem), and repelleted. Lysates were made by glass bead cell disruption (3–5 cycles, 1 min each), with intermittent cooling on ice, in buffer that contained 100 mM KCl, 2 mM magnesium acetate, 20 mM HEPES-KOH, pH 7.4, 14.4 mM β-mercaptoethanol, 100 μg/ml cycloheximide. Cell debris was removed by centrifugation at 7000 rpm for 8 min. Ribosomes were resolved in 10–25% sucrose gradients containing 100 mM KCl, 5 mM MgCl<sub>2</sub>, 20 mM HEPES-KOH, pH 7.4, and 2 mM dithiothreitol (Beckman SW28 rotor, 20,000 rpm, 19.5 h). Gradients were collected with continuous monitoring at 254 nm using an ISCO UA-5 absorbance detector and 1640 gradient collector. Proteins collected from sucrose gradient fractions were precipitated with 10% trichloroacetic acid and resolved in 10% Laemmli SDS-polyacrylamide gel electrophoresis and transferred onto Immobilon (Millipore Corp.) membranes.

**Western Blotting**—Western blotting was performed following standard procedures (22). For studying *eIF2A* time course degradation experiments, yeast extracts were obtained by glass beads disruption of the yeast cells mixed with protein loading buffer. After vigorous vortexing, the beads and cell debris were removed by centrifugation at 14,000 rpm for 5 min, and Western blots were decorated with either mouse monoclonal anti-HA tag antibodies (Cell Signaling, Inc.) or with custom made rabbit anti-*eIF2A* antibodies followed by incubation with either goat anti-mouse or goat anti-rabbit horseradish peroxidase-conjugated antibodies. The antibodies for actin and phosphoglycerate kinase were obtained from



Santa Cruz Biotechnology, Inc. (Santa Cruz, CA). The blots were then detected with an ECL™ kit (Amersham Biosciences).

**Expression and Purification of a Recombinant *eIF2A* Protein Fragment**—*eIF2A* cDNA fragment (comprising residues Gly<sup>59</sup>–Glu<sup>420</sup>) was amplified by PCR using 5'-AACGCGATCCGGTCCATGTTGGATA-ACGTTCTATTAAC-3' as an upstream primer and 5'-TTCCGGAATT-CCTCTTAACAAATACTAAAGAGCCTGATACATGC-3' as a downstream primer, digested with BamHI and EcoRI, and cloned into pMW-127 vector (23, 24) as a fusion to the gene encoding staphylococcal nuclease bearing on its N-terminal end a His<sub>6</sub> tag. The plasmid was transformed into BL21-CodonPlus (DE3)-RIL (Stratagene) cells. Cells were grown at 37 °C to an A<sub>600</sub> of 0.6, induced with 1 mM isopropyl-β-D-thiogalactoside, harvested by centrifugation after 3 h of induction, and lysed by sonication in 20 mM Tris/HCl, pH 8.0, buffer, containing complete EDTA-free protease inhibitor mixture tablets (Roche Applied Science). The recombinant protein was found to be insoluble and was further purified from the inclusion bodies under denaturing conditions (6 M urea, 20 mM Tris/HCl, pH 8.0, 0.5 M NaCl, 10 mM imidazole, 1 mM β-mercaptoethanol) on a Ni<sup>2+</sup>-nitrilotriacetic acid beads following standard procedures described elsewhere. After the Ni<sup>2+</sup>-nitrilotriacetic acid column purification, the protein was found to be 95–97% pure and was then dialyzed against 10 mM Tris/HCl buffer, pH 7.5, containing 0.2% SDS, 1 mM EDTA, and 10 mM β-mercaptoethanol and concentrated using an Ultrafree-15 centrifugal filter device (Millipore Corp.) and further used for immunization of rabbits. Rabbit polyclonal antibodies were produced by United States Biological, Inc.

**Actin Phalloidin Staining**—Yeast strains were grown in YEPD medium for 16 h in log phase by continual dilution at 30 °C. Fixation was performed by adding formaldehyde and Triton X-100 to a final concentration of 4 and 0.5%, respectively, and incubated for 30 min at room temperature. Yeast pellets were resuspended in PBS buffer plus 0.5 mM MgCl<sub>2</sub> and 4% formaldehyde for further fixation for 90 min at room temperature. Cells were washed once with PBS prior to phalloidin addition to a final concentration of 0.6 μM in PBS and incubated for 60 min at room temperature in the dark. Yeast samples were subsequently washed three times with PBS and resuspended in 1× mounting medium (90% glycerol, 0.1% PBS, 92 mM *p*-phenylenediamine). Images were captured with an IX70 inverted fluorescence microscope (Olympus) equipped with a HiQ fluorescein filter set (excitation wavelength: 450–492 nm); a Planapochromatic 100× oil immersion objective lens; and a 100-watt mercury lamp. Images were collected and analyzed with a Princeton Instruments 5-MHz MicroMax cooled CCD camera, a shutter and controller unit, and IPLab software (version 3.5; Scanalytics).

**Flow Cytometry**—Yeast strains were grown in YEPD medium for 16 h in log phase by continual dilution at 30 °C. Fixation was performed by adding ethanol to a final concentration of 70% and incubation overnight at 4 °C. Yeast pellets were resuspended in 50 mM sodium citrate (pH 7.0) and digested with RNase I (0.25 mg/ml) for 1.5 h at 50 °C. Samples were washed three times with 50 mM sodium citrate (pH 7.0) before suspension in this buffer with 16 μg/ml propidium iodide. Samples were analyzed on a Coulter Cytomics FC500 flow cytometer.

**Miscellaneous**—Molecular cloning was performed following the general procedures described by Sambrook *et al.* (25). DNA sequencing was accomplished by the Molecular Biology Core Laboratory at Case Western Reserve University. Sequencing was performed with custom synthesized oligonucleotides using the fluorescently labeled dideoxymethodology. SDS-PAGE was performed according to either the Laemmli (26) or Schagger and von Jagow (27) procedures. Yeast genomic DNA was isolated using the DNA-Pure™ Yeast Genomic Kit from CPG, Inc., following the manufacturer's protocol. β-Galactosidase activity was measured following the protocol described by Clontech (59) with *o*-nitrophenyl β-D-galactopyranoside as a substrate. Cell extracts were prepared by subsequent cycles of cell freezing in liquid nitrogen and thawing at 37 °C.

## RESULTS

The *eIF2A* null mutant has been shown to have no apparent phenotype in a variety of systematic tests assaying growth, metabolism, cell cycle progression, cytoskeleton and mitochondrial morphology, mating, stability of an artificial minichromosome, rate of spontaneous mutation, etc. (14, 28, 29), although it was found to possess reduced sporulation efficiency (14). We have, however, previously shown that the double *2Δ/5Δ* mutant is “synthetically sick.” This suggested a genetic interaction between *eIF2A* and *eIF5B* (14). To further investigate the cellular functions of *eIF2A* in *Saccharomyces cerevisiae*, we

decided to look for other initiation factors that could possibly genetically interact with *eIF2A*. Such genetic relationships, if they exist, suggest a functional interaction between the corresponding gene products. However, disruption of the vast majority of the initiation factors in yeast is known to be lethal. Thus, we decided to take advantage of combining the *eIF2A* mutation with some of the yeast temperature-sensitive mutants carrying *ts* mutations in the respective initiation factors. As a first step in this line of reasoning, the *eIF2A* gene (open reading frame *YGR054W*) was disrupted in the *eIF4E-ts* strain 4-2 using the kanMX disruption module and the resulting *eIF4E-ts* strain 4-2/2A (*MATa*, *ade2-1*, *leu2-3,112*, *his3-11,15*, *trp1-1*, *ura3*, *ygr054w::KanMX*, *cdc33::LEU2* <*cdc33-4-2*; *TRP1*, *ARSCEN*>) was obtained.

**The *eIF4E-ts* Strain with a Disrupted Copy of the *eIF2A* Gene Is Synthetically Sick and Displays an Altered Phenotype**—*eIF4E-ts* strain 4-2 has two point mutations in the *eIF4E* gene, which confer a temperature-sensitive phenotype, resulting in a rapid shutoff of protein synthesis and cell growth at the non-permissive temperature (37 °C) (15). However, at permissive temperatures (28–30 °C), this strain displays growth rates that are only slightly reduced (15).

Surprisingly, the double *eIF4E-ts* and *eIF2A* mutant strain revealed a severe slow growth phenotype (Fig. 2A) when compared with the parental strains. The doubling time for this strain at 28 °C in liquid YPD glucose medium was found to be ~4–4.2 h, whereas for the *eIF4E-ts* strain, it is about 2.5 h. This severe slow growth phenotype can be reverted by reintroducing the *eIF2A* gene on a CEN plasmid (Fig. 2A). Mutations in the *eIF4E* (*CDC33*) gene are known to arrest yeast cells at random points in the cell cycle (30, 31). To determine whether the *eIF4E-ts/eIF2AΔ* null mutant also presents a defect in cell cycle progression, we analyzed all strains by flow cytometry. At 30 °C, the *eIF4E-ts* 4-2 strain showed an increased cell population in G<sub>2</sub> (73% total) (Fig. 2B). This effect was further exaggerated to more than 82% in *eIF4E-ts/eIF2AΔ* null mutant cells (Fig. 2B), perhaps contributing to the synthetic slow growth phenotype observed (Fig. 2A).

The 4-2/2A strain also displayed an altered phenotype (cell morphology) in comparison with ancestor *eIF4E-ts* strains 4-2 and WT CWO4 (Fig. 2C). On average, the 4-2/2A cells were larger in size and more rounded in shape, representing almost perfect circles (Fig. 2C). The establishment of cell morphology is universal during the development of both uni- and multicellular organisms (32). Wild type yeast cells have a relatively simple ellipsoidal shape; however, a number of mutants with elongated, round, small, large, pointed, clumped, and other shapes have been reported (33). In general, yeast cell growth and morphogenesis is a complex process, which is tightly linked to the cell cycle (34). The organization of the actin cytoskeleton plays a critical role in this morphogenic process (35). It is therefore possible that in the double *eIF4E-ts* and *eIF2A* mutant strain, the expression and/or organization of the actin cytoskeleton is affected. To check the latter, the actin cytoskeleton from the different yeast strains was stained using rhodamine phalloidin, and the samples were analyzed by fluorescence microscopy (Fig. 2D). The parental strains CWO4 and BY4741 revealed similar actin cytoskeleton organization, where actin cables were generated from the buds and along the cytoplasm, showing correct polarization toward regions of cell growth (Fig. 2D and data not shown). Actin cytoskeleton organization in the *eIF4E-ts* strain was somewhat altered with a partial loss of actin cables and depolarization. In contrast to CWO4 and *eIF4E-ts* strains, cytoskeletal organization, and polarization in the *eIF4E-ts* and *eIF2A* double mutant strain was severely affected, with almost complete disruption of the actin

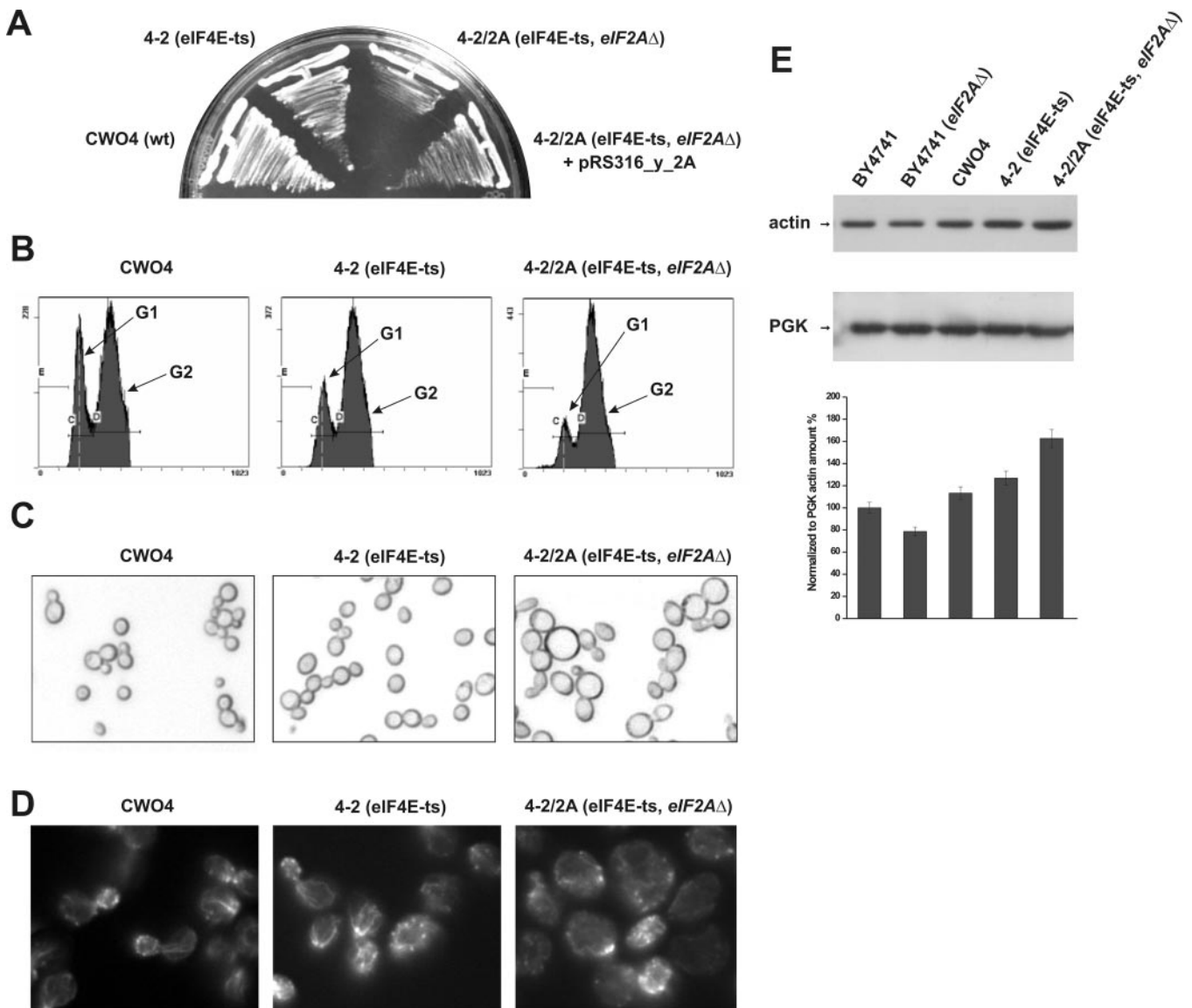


**FIG. 2. Mutant *eIF4E-ts* yeast strain 4-2/2A with a disrupted copy of the *eIF2A* gene displays a severe slow growth phenotype.** *A*, yeast cell growth. Cells were grown for 36 h on a solid YEPD agar medium containing 2% glucose. *B*, cell cycle distribution. DNA samples collected from different yeast strains grown for 16 h on liquid YEPD were analyzed by flow cytometry after propidium iodide staining using a Coulter Cytomics FC500 Flow Cytometer. *C*, yeast cell morphology. Cells were scraped off of the plate and resuspended in 10  $\mu$ l of water onto microscope slides. Images were taken using a Zeiss TELAVAL 31 microscope equipped with a Spot Diagnostic Instrument Inc. digital camera at  $\times 40$  magnification. *D*, yeast actin cytoskeleton staining with phalloidin. Yeast strains grown in YEPD medium for 16 h in log phase were fixed and stained with rhodamine phalloidin prior to mounting. Images were captured with an IX70 Olympus inverted fluorescence microscope equipped with a Planapochromatic  $\times 100$  oil immersion objective lens. *E*, levels of the actin protein. Cells were grown in YEPD medium for 16 h (log phase) and collected, and proteins were extracted. Subsequently, proteins were resolved by SDS-PAGE with the proteins then transferred to cellulose membranes and probed with antibodies to actin or phosphoglycerate kinase (for loading control). Densitometry analysis was performed using the Amersham Biosciences software ImageQuant 5.2, and intensity of the signal was corrected against phosphoglycerate kinase blots and expressed as a percentage of control (BY4741 strain).

cytoskeleton resulting in a total loss of the actin cables and almost complete depolarization (Fig. 2*D*). It should be noted, however, that no change in actin cytoskeleton organization was observed in the single *eIF2A $\Delta$*  mutant strain (data not shown).

To determine whether actin expression was altered at the protein level, cell extracts were prepared and Western blots for actin were performed. To our surprise, it was found that actin levels were not constant in all samples. Strains carrying the *eIF4E-ts* mutation presented an increase in actin protein when compared with its wild type counterpart (30% increase), and the double *eIF4E-ts* and *eIF2A* mutant strain presented even greater changes with more than a 50% increase in actin levels (Fig. 2*E*). Thus, *eIF2A* might have a critical function in yeast in controlling (under certain specific conditions) the expression of

the genes involved in cytoskeleton formation and assembly and this could ultimately lead to a change of cell morphology.

The observed genetic interaction of *eIF2A* and *eIF4E* suggests that both proteins function in the same pathway, namely initiation of protein synthesis. However, we have previously shown that *eIF2A* does not affect cap-dependent initiation or reinitiation in yeast as monitored using various *GCN4-lacZ* fusion constructs (kindly provided by Dr. Thomas Dever, National Institutes of Health) (14).

It was, however, still possible that *eIF2A* might affect internal initiation. To study the effect of *eIF2A* on IRES-mediated expression in yeast, the *Ure2p-lacZ* reporter system was used (20). In this construct, the *URE2* IRES (*URE2* open reading frame amino acids 3–353) was inserted in frame with *lacZ* and

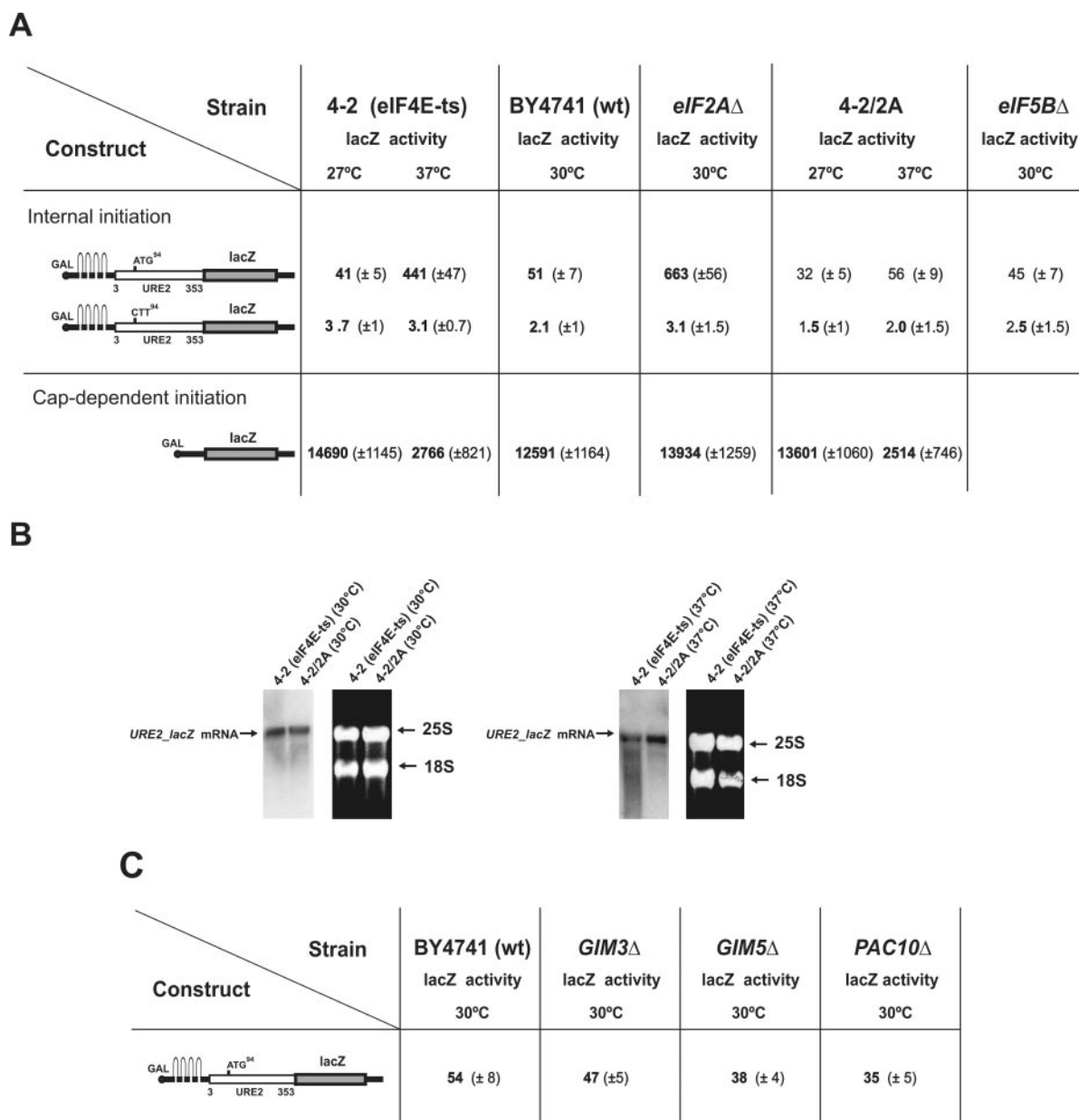


**FIG. 3. Activity of the *Ure2p* IRES is up-regulated in yeast strains carrying *eIF4E-ts* and/or *eIF2A*Δ mutations.** *A*, expression of reporter constructs under the control of the *GAL1/10* promoter transformed into *eIF4E-ts* strain 4-2 or isogenic wild-type BY4741, *eIF2A*Δ, and *eIF5B*Δ strains. Activity in the mutant *eIF4E-ts* strain 4-2/2A is also shown.  $\beta$ -Galactosidase activity (relative units) was determined following the protocol described by Clontech (59) after a 20-h induction of the cells in 2% galactose at the indicated temperature. *B*, Northern blot analysis of *Ure2p-lacZ* mRNA expressed in *eIF4E-ts* strain 4-2 or isogenic 4-2/2A strain. For each lane, 25  $\mu$ g of total yeast RNA was separated on a denaturing agarose gel, transferred onto a BrightStar™-Plus Nylon membrane (Ambion), and hybridized to a  $^{32}$ P-labeled DNA *lacZ* probe. rRNA loading controls are shown to the right of the Northern blots. *C*, *Ure2p* IRES activity in isogenic WT BY4741 and *GIM3*Δ, *GIM5*Δ, and *PAC10*Δ mutant strains ( $\beta$ -galactosidase activity was measured as above).

placed behind a stable hairpin structure ( $> -30$  kcal/mol). This hairpin structure reduces cap-dependent *lacZ* expression almost completely (20, 36). Two constructs were produced; they carried at position 94 either ATG-Met (internal initiation start) or CCT-Leu (ATG was mutated to CCT in order to abolish internal initiation, used as a negative control) (20). Although there was almost no expression from the CCT-Leu construct, there was a significant increase in the level of  $\beta$ -galactosidase expressed in an *eIF4E-ts* strain at the nonpermissive temperature (37 °C) compared with expression in wild type cells, indicating that the expression from the *URE2* IRES is *eIF4E*- and cap-independent (Fig. 3) (20).

**Expression from the *URE2* IRES Is Up-regulated in Yeast Cells Lacking *eIF2A***—Surprisingly, it was found that *lacZ* expression driven by the *URE2* IRES was plasmidally enhanced

in the *eIF2A* null strain in comparison with the WT strain having the same genetic background and that the observed increase in the activity was even greater than that measured for the *eIF4E-ts* strain at the nonpermissive temperature (Fig. 3A). At the same time as it was noted before (14), cap-dependent initiation in the *eIF2A*Δ strain was not significantly affected, although a slight increase in its level was observed (Fig. 3A) when using a construct encoding *lacZ* mRNA with a 5'-untranslated region derived from the *GAL1* gene (19). Surprisingly, we also found that the activity of *URE2* IRES was not up-regulated in the double *eIF4E-ts* and *eIF2A* mutant strain at the permissive temperature and was only slightly elevated at the nonpermissive temperature (Fig. 3A), suggesting that expression of some other genes required for efficient *URE2* IRES utilization may have also been affected in this strain. It



TABLE I  
Strains of *S. cerevisiae* used in this study

Strain	Genotype	Source
CWO4	<i>MATa, ade2-1, leu2-3,112, his3-11,15, trp1-1, ura3</i>	P. Linder
4-2	<i>MATa, ade2-1, leu2-3,112, his3-11,15, trp1-1, ura3, cdc33::LEU2 &lt;cdc33-4-2; TRP1, ARSCEN&gt;</i>	M. Altmann
4-2/2A	<i>MATa, ade2-1, leu2-3,112, his3-11,15, trp1-1, ura3, ygr054w::KanMX, cdc33::LEU2 &lt;cdc33-4-2; TRP1, ARSCEN&gt;</i>	This work
BY4741	<i>MATa, his3-1, leu2-0, met15-0, ura3-0</i>	Research Genetics
BY4741 ( <i>eIF2AΔ</i> )	<i>MATa, his3-1, leu2-0, met15-0, ura3-0, ygr054w::KanMX</i>	Research Genetics
BY4741 ( <i>eIF5BΔ</i> )	<i>MATa, his3-1, leu2-0, met15-0, ura3-0, fun12::KanMX</i>	Research Genetics
BY4741 ( <i>GIM3Δ</i> )	<i>MATa, his3-1, leu2-0, met15-0, ura3-0, gim3::KanMX</i>	T. Dever
BY4741 ( <i>GIM5Δ</i> )	<i>MATa, his3-1, leu2-0, met15-0, ura3-0, gim5::KanMX</i>	T. Dever
BY4741 ( <i>PAC10Δ</i> )	<i>MATa, his3-1, leu2-0, met15-0, ura3-0, pac10::KanMX</i>	T. Dever
H2879	<i>MATa, leu2-3, leu2-112, ura3-52, PRT1</i>	T. Dever
H1676	<i>MATa, leu2-3, leu2-112, ura3-52, prt1-1</i>	T. Dever

should be noted that no reduction of *URE2 lacZ* mRNA levels in the double 4-2/2A mutant strain in comparison with the *eIF4E-ts* strain 4-2 (at both permissive and nonpermissive temperatures) was observed that could account for the observed differences in *URE2* IRES activity (Fig. 3B). Also, the level of cap-dependent initiation and the extent of its inhibition at the nonpermissive temperature in 4-2/2A strain was found to be very similar to that of *eIF4E-ts* strain 4-2 (Fig. 3A). In both cases an ~5-fold reduction in the expression of *lacZ* reporter driven by cap-dependent initiation was observed. Since eIF2A was also found to genetically interact with *GIM3*, *GIM5*, and *PAC10* genes (members of the prefoldin complex) (37), we also tested whether mutations in these genes could affect the activity of the *URE2* IRES. No apparent change in *URE2* IRES activity was observed when comparing isogenic *GIM3*, *GIM5*, and *PAC10* null mutants and the WT BY4741 strain (Table I, Fig. 3C). It was concluded that up-regulation of *URE2* IRES in eIF2A null strain could primarily be related to the activity of eIF2A protein.

**Expression of eIF2A Down-regulates URE2 IRES Activity in Yeast Cells**—To further address the possibility that eIF2A functions as a suppressor of Ure2p IRES-mediated translation initiation, the yeast eIF2A gene was reintroduced into the eIF2A knockout yeast strain expressing the Ure2p-*lacZ* fusion construct. eIF2A was expressed either from its own promoter in a YCplac111 plasmid (Fig. 4A) or as an HA-tagged eIF2A expressed from the *GAL* promoter in the pTB328 plasmid. In both cases, down-regulation of *URE2* IRES activity was observed (Fig. 4A); however, overexpression of eIF2A from the *GAL* promoter down-regulated *URE2* IRES activity more efficiently. The eIF2A knockout strain transformed with either the pTB328 or YCplac111 plasmids was used as a control, and no down-regulation of *URE2* IRES activity was observed in the latter cases. Also tested was whether human eIF2A (which is 28% identical and 58% similar to the yeast protein in amino acid sequence) could substitute for its yeast homologue *in vivo*. It was found that human HA-tagged eIF2A can also suppress the expression from the *URE2* IRES element, but it functions about 60% as well as yeast HA-tagged eIF2A in repressing the expression of *lacZ* (Fig. 4A). Both yeast and human proteins were found to be associated with 40 and 80 S ribosomes; however, association of the human protein with 80 S ribosomes was significantly reduced (Fig. 4B), and in contrast to the yeast protein, the human homologue was found predominantly associated with 40 S ribosomes. We anticipate that the reduced association of human eIF2A with 80 S ribosomes could account for its reduced ability to suppress expression from the *URE2* IRES element (by comparison with the yeast protein).

It should be noted that no apparent change in *URE2 lacZ* mRNA levels was observed when comparing WT yeast, yeast *eIF2A* knockout, and yeast *eIF2A* knockout strains transformed with either yeast or human eIF2A that could account

for the observed difference in *lacZ* activity (Fig. 4C). Thus, it was concluded that eIF2A functions as a negative regulator of Ure2p IRES-mediated expression. Interestingly, only a 2-fold reduction of *URE2* IRES activity was observed in the WT strain when overexpressing HA-tagged yeast eIF2A. This could indicate that under the experimental conditions used, eIF2A is present in wild-type yeast cells at sufficiently high concentrations such that an increase in eIF2A levels does not further reduce expression from the Ure2p IRES element.

**Association of eIF2A with 40 and 80 S Is Not Impaired in the FUN12Δ (eIF5BΔ) Strain**—We have previously shown the genetic interaction between eIF2A and eIF5B (14). eIF5B was also known to interact with eIF2A in the process of 80 S complex formation in a reconstituted system when using AUG codon (7). We decided to check whether the presence of eIF5B affected the binding of eIF2A to either 40 or 80 S ribosome *in vivo* in yeast cells. The HA-tagged eIF2A was transformed into an isogenic WT strain BY4741 (*MATa, his3-1, leu2-0, met15-0, ura3-0*) and *eIF5BΔ* (*MATa, his3-1, leu2-0, met15-0, ura3-0, fun12::KanMX*), and we found that similar amounts of HA-tagged eIF2A were present in the 40 and 80 S ribosomes of the WT and *eIF5BΔ* strains (Fig. 5A). It was concluded that the absence of eIF5B does not affect binding of eIF2A to 40 and 80 S ribosomes. If, as we hypothesized, suppression of IRES activity through eIF2A protein in yeast cells occurs at the level of 40 S/80 S ribosomes, one would then expect that there will be no change in *URE2* IRES activity in *eIF5BΔ* cells. Indeed, as expected, we observed no difference in *lacZ* expression driven by *URE2* IRES in *eIF5BΔ* cells in comparison with WT yeast cells (Fig. 3A).

**eIF2A Remains Bound to 40 and 80 S Subunits in Extracts of prt1-1 Cells Incubated at the Nonpermissive Temperature**—The *prt1-1* mutation replaces Ser<sup>518</sup> with Phe in the Prt1p (eIF3b) subunit of yeast eIF3 and confers a ts phenotype. Incubation of *prt1-1* cells at the nonpermissive (37 °C) temperature produces a run-off of polysomes and accumulation of 80 S monosomes (38). We asked whether incubating *prt1-1* cells at the nonpermissive temperature would change the amount of eIF2A associated with 40 S/80 S subunits. We found that eIF2A remained bound to 40 and 80 S subunits in the *prt1-1* cells at the nonpermissive temperature and that the amount of eIF2A bound to 80 S ribosomes increased slightly with the accumulation of 80 monosomes at the nonpermissive temperature (Fig. 5B, right).

**eIF2A Is an Inherently Unstable Protein**—From the Stanford yeast genome expression connection data base (available on the World Wide Web at genome-www.stanford.edu/yeast\_stress/), it is known that the mRNA levels for eIF2A are highest under optimal growth conditions and decrease 2–8-fold under a wide variety of stress conditions, including heat shock, nitrogen depletion, amino acid starvation, diauxic shift, and stationary phase among others. We hypothesize that the decrease in eIF2A mRNA levels would be accompanied by a decrease in

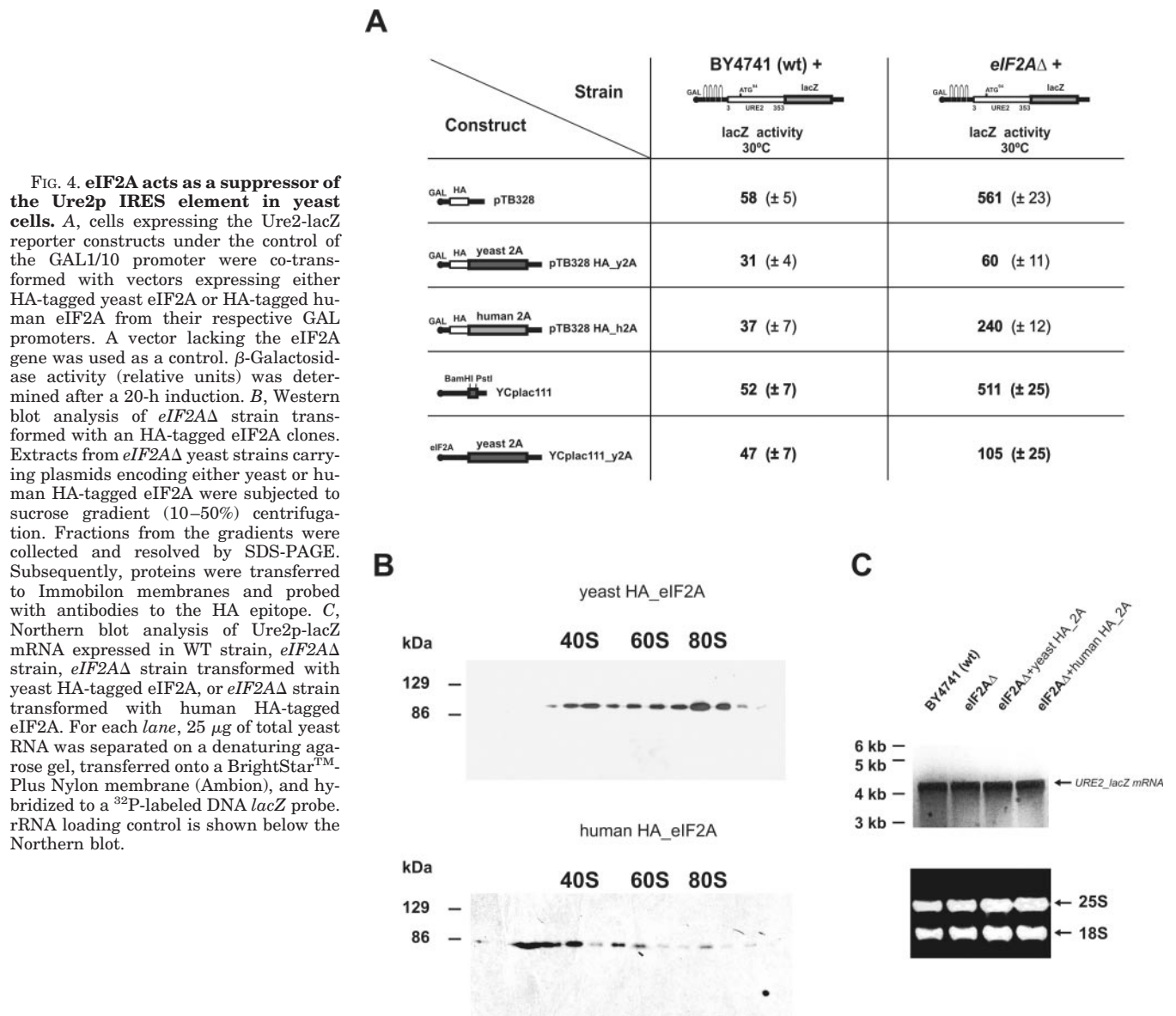


**FIG. 4. *eIF2A* acts as a suppressor of the *Ure2p* IRES element in yeast cells.** *A*, cells expressing the *Ure2-lacZ* reporter constructs under the control of the *GAL1/10* promoter were co-transformed with vectors expressing either HA-tagged yeast *eIF2A* or HA-tagged human *eIF2A* from their respective *GAL* promoters. A vector lacking the *eIF2A* gene was used as a control.  $\beta$ -Galactosidase activity (relative units) was determined after a 20-h induction. *B*, Western blot analysis of *eIF2A*Δ strain transformed with an HA-tagged *eIF2A* clones. Extracts from *eIF2A*Δ yeast strains carrying plasmids encoding either yeast or human HA-tagged *eIF2A* were subjected to sucrose gradient (10–50%) centrifugation. Fractions from the gradients were collected and resolved by SDS-PAGE. Subsequently, proteins were transferred to Immobilon membranes and probed with antibodies to the HA epitope. *C*, Northern blot analysis of *Ure2p-lacZ* mRNA expressed in WT strain, *eIF2A*Δ strain, *eIF2A*Δ strain transformed with yeast HA-tagged *eIF2A*, or *eIF2A*Δ strain transformed with human HA-tagged *eIF2A*. For each lane, 25  $\mu$ g of total yeast RNA was separated on a denaturing agarose gel, transferred onto a BrightStar<sup>TM</sup>-Plus Nylon membrane (Ambion), and hybridized to a <sup>32</sup>P-labeled DNA *lacZ* probe. rRNA loading control is shown below the Northern blot.

*eIF2A* protein levels. To address this question, we monitored the levels of HA-tagged *eIF2A* (which is under the control of the *GAL* promoter) by immunoblotting with anti-HA antibodies and compared them with the level of HA-tagged *eIF4E* (placed also under the control of the *GAL* promoter). A similar approach was used to address the question of cyclin 2 stability in yeast cells and was proven to be appropriate (39). Both HA-tagged *eIF2A* and HA-tagged *eIF4E* constructs were transformed into the *eIF2A*Δ strain, and the levels of HA-tagged proteins were monitored in the presence of galactose and then subsequently following transfer to glucose. Repression, acting through the upstream repression sequence element in the *GAL* promoter, is established rapidly, within a few min of glucose addition, leading to an immediate cessation of the galactose-dependent mRNA synthesis (40). Thus, it was possible to determine the half-life of HA-tagged *eIF2A* under the conditions where there was no continued synthesis of *eIF2A* protein. By Western blotting with an HA antibody, it was found that the levels of HA-tagged *eIF2A* and *eIF4E* are about the same when cells are grown on galactose (Fig. 6, *A*, *C*, and *D*). Upon transfer to glucose, the levels of HA-tagged *eIF4E* remained unchanged for about 1.5–2 h, whereas the levels of HA-tagged *eIF2A* were rapidly reduced with an estimated half-life of 17–18 min. The

lack of a drop in signal in the case of the HA-tagged *eIF4E* reflects, in part, a lag in the growth curve for the yeast in their adaptation to growth on glucose (*i.e.* there is no apparent change in  $A_{600}$  until roughly 2 h following the switch to glucose (Fig. 6*B*)). With more extended periods of time, there is the expected decrease in HA-tagged *eIF4E* concomitant with the increase in cell number (*i.e.* a dilution effect; data not shown). In contrast to HA-tagged *eIF4E*, a rapid drop-off in the signal for HA-tagged *eIF2A* was observed, suggesting that HA-tagged *eIF2A* is an inherently unstable protein. We used an HA epitope tag for detection, since the monoclonal antibodies against HA epitope are extremely sensitive, allowing one to detect very low levels of the tagged protein. One caveat to this experiment is that the observed instability of HA-tagged *eIF2A* could be apparent and might result from the rapid cleavage of the HA epitope. To verify our conclusion, we also used a polyclonal antibody derived against the central core fragment (Gly<sup>59</sup>–Glu<sup>420</sup>) of the recombinant *eIF2A* and measured the half-life of the HA-tagged *eIF2A* after repression of the *GAL1* promoter by glucose. A similar decay of the *eIF2A* signal was observed (Fig. 6*F*).

Interestingly, a strong proline, glutamic acid, serine, threonine (PEST) motif (41, 42) of 24 amino acids (KSSETSPDST-

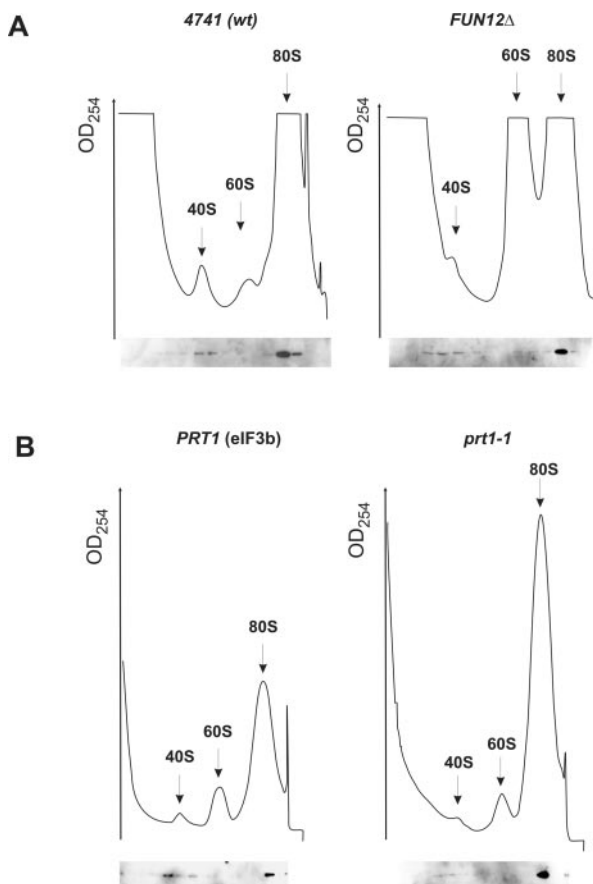


**FIG. 5. Ribosome profile and Western blot analysis of the yeast strains transformed with an HA-tagged *eIF2A* clone.** *A*, extracts from WT BY4741 (*left*) and isogenic *eIF5B* $\Delta$  (*right*) yeast strains carrying a plasmid encoding the wild type HA-*eIF2A* under control of a galactose inducible promoter were subjected to sucrose gradient (10–25%) centrifugation. *B*, extracts from isogenic PRT1 (H2879) and *prt1-1* (H1676) cells (carrying the same plasmid encoding the wild type HA-*eIF2A* under control of a galactose-inducible promoter) grown in YPD medium at 28 °C and treated for 15 min at 37 °C were subjected to sucrose gradient (10–25%) centrifugation. Each fraction from the gradient was precipitated with cold 10% trichloroacetic acid, resuspended in SDS sample buffer, and subjected to electrophoresis. Subsequently, proteins were transferred to Immobilon membranes and probed with the monoclonal antibodies to the HA epitope.

PAPSAPASTNAPTNNK) exists between positions 559 and 584 of the *eIF2A* amino acid sequence with a PEST score of 16.12 calculated using the PEST-FIND program (available on the World Wide Web at [www.hgmp.mrc.ac.uk/Software/EMBOSS/Apps/pestfind.html](http://www.hgmp.mrc.ac.uk/Software/EMBOSS/Apps/pestfind.html)) originally developed by Scott Rogers and Martin Rechsteiner in 1986. It is widely believed that PEST sequences are responsible for rapid degradation of proteins containing this motif, and a PEST score of more than 5 denotes a very strong proteolytic degradation signal (41, 42). *eIF2A* is also found to be among 1075 proteins identified as yeast ubiquitin conjugates (43). Ubiquitinated proteins are well known to be substrates for rapid turnover (44). This was not the case for *eIF4E* or any of the three subunits of initiation factor *eIF2* (43). It should be noted that no significant difference in the levels of the two mRNAs was observed as determined by Northern blotting, and both mRNAs were almost completely degraded after 20 min following the switch from galactose to glucose (Fig. 4E).

#### DISCUSSION

Genetic analyses have proven to be a powerful tool for elucidating the biological function of proteins in *S. cerevisiae*, and *eIF2A* has now appeared in several genetic screens (14, 37). First, it was shown to genetically interact with *eIF5B* (14). This

suggests that both proteins function in the same pathway (14). Although our experiments with *FUN12* $\Delta$  strain did not support the idea of a direct physical interaction of these two proteins *in vivo* during binding to 40 S/80 S ribosomes, they did not exclude the possibility that this interaction could be through some other protein or the ribosome either. Indeed, genetically interacting genes do encode proteins often found in the same complex, however, global analyses have shown that only 30 of 4039 genetically interacting gene pairs in *S. cerevisiae* encode physically interacting proteins (37). Very recently, *eIF2A* was also found to genetically interact with the members of the prefoldin complex, *GIM3*, *GIM5*, and *PAC10* (37). The double knockouts of *eIF2A/GIM3*, *eIF2A/GIM5*, and *eIF2A/PAC10* mutants display a severe slow growth phenotype (37). Members of the *GIM* family in yeast are important for the folding of tubulin and actin (45). Prefoldin binds ribosome-associated actin chains after synthesis of the first ~145 amino acids and remains bound to the actin polypeptide until its posttranslational delivery to the cytosolic chaperonin (46). Members of the prefoldin complex in contrast to *eIF2A* are predominantly associated with polysomes and not with 40 S/80 S ribosomes (46). The rapid assembly and disassembly of actin and tubulin filaments at specific subcellular locations provides the mechanistic basis for various dynamic activities such as segregation of chromosomes, change of cell shape/morphology, translocation of intracellular organelles, and others (47). Although none of the above mentioned genes have an obvious direct relationship with the translation process, this observation provides additional evidence that *eIF2A* might have a critical function in yeast in controlling (under certain specific conditions) the expression of the genes involved in cytoskeleton formation and assembly, and this could finally lead to a change of cell morphology. Our findings that the *eIF4E-ts/eIF2A* $\Delta$  yeast strain displays altered actin organization when compared with the parental strains as well as an affected morphogenic processes supports this suggestion. The significant increase in actin levels observed in the *eIF4E-ts/eIF2A* $\Delta$  strain may be the cause of a slow growth phenotype. Remarkably, overexpression of actin is lethal in yeast; however, the reason for this sensitivity is not well understood (48, 49). It is unclear which gene expression is affected in the 4-2/2A strain that subsequently causes the observed changes in cell shape, actin disorganization, and actin levels. However, the genetic interaction of *eIF4E* and *eIF2A* reported here clearly shows that both proteins function in the same pathway.

It should be noted that translational control of gene expression has become the focus of many studies during the last 10 years. Recent studies have led to an increase in our understanding of how the balance between different initiation mechanisms (namely cap-dependent initiation, leaky scanning, reinitiation, and internal initiation) might influence cell fate (3–5, 50). This can be accomplished through the mechanisms that target specific initiation factors (altering their activity, affecting their integrity or protein levels). So far, initiation factors *eIF4E*, *eIF4G*, *eIF2*, and *eIF2B* have proven to be the main targets for translational control (51–55). In general, their inactivation is triggered by stress and their activation by growth proliferation signals. A part of the overall effect of stress is the decrease in cap-dependent translation through a reduction of *eIF4F* activity. At the same time, however, many mRNAs continue to be translated or become more efficiently translated under these conditions (56). These mRNAs are the most competitive, cap-dependently translated mRNAs or those mRNAs that are internally initiated (IRES containing).

In the past few years, IRES elements have been detected in an increasing number of cellular mRNAs from various species



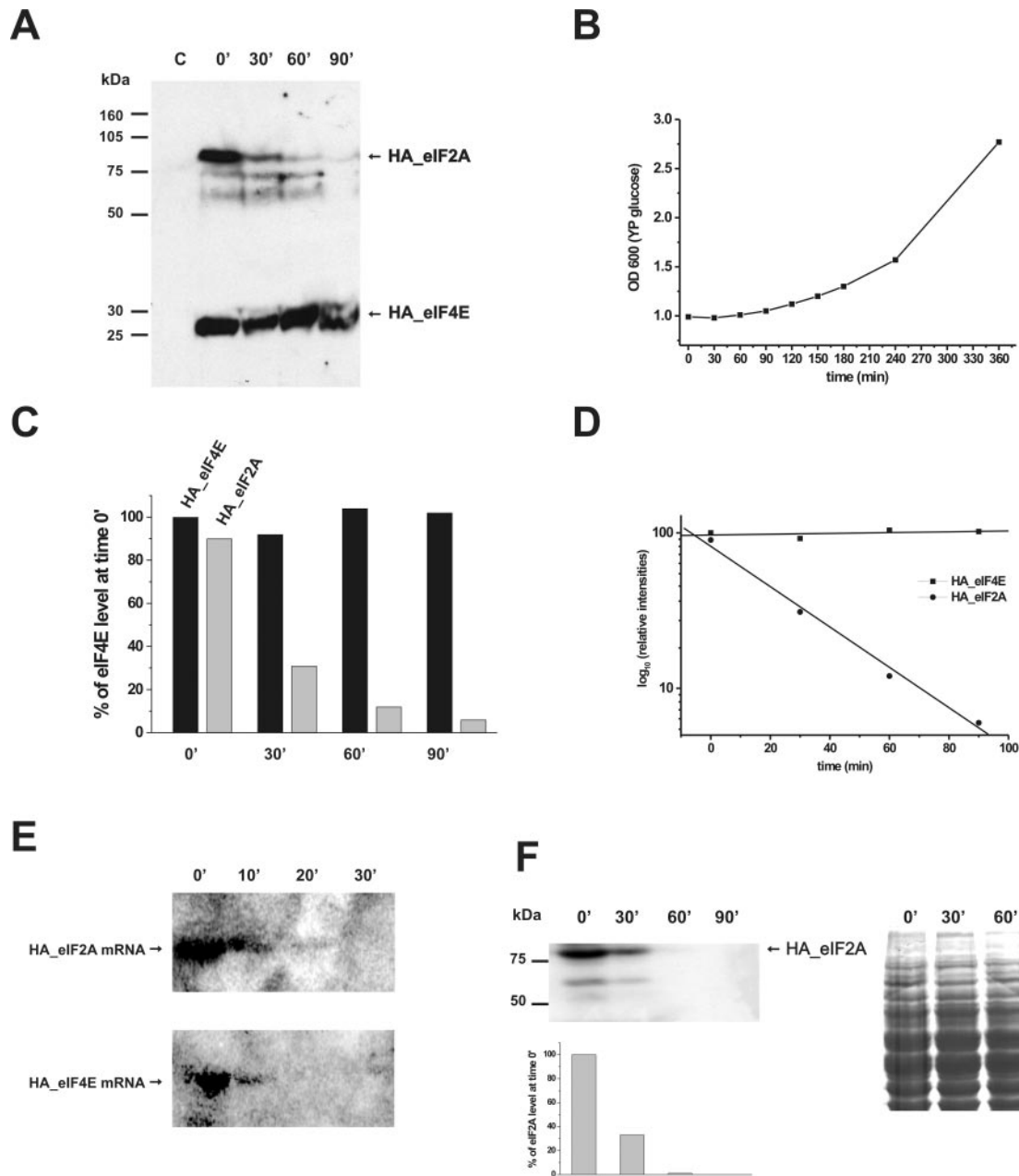


**FIG. 6. Yeast *eIF2A* is unstable protein.** *A*, *eIF2A* $\Delta$  yeast cells co-transformed with HA-tagged *eIF2A* and HA-tagged *eIF4E* expression plasmids were grown overnight (18 h) on galactose YP-rich medium to allow for the expression of both HA-tagged *eIF2A* and HA-tagged *eIF4E* from their respective GAL promoters. Yeast cells co-transformed with ancestor plasmids that do not contain either *eIF2A* or *eIF4E* genes were used as control (lane C). At time 0, the cells were washed with water and then resuspended in YP medium containing glucose. Aliquots (50 ml) of the cells were taken at the indicated times. The yeast were pelleted and then dissolved in 200  $\mu$ l of 20 mM HEPES/KOH buffer (pH 7.4) containing 100 mM KCl, 2 mM MgAc, 14.4 mM  $\beta$ -mercaptoethanol, 100  $\mu$ g/ml cycloheximide. The cells were lysed by subsequent cycles of freezing in liquid nitrogen and thawing at 37  $^{\circ}$ C, and insoluble material was pelleted by centrifugation. Approximately equal amounts of protein from the supernatants were subjected to SDS Tris/Tricine 11.5% acrylamide gel electrophoresis. Proteins were transferred to nitrocellulose membranes and probed with anti-HA antibodies (Santa Cruz Biotechnology). *B*, yeast cell growth ( $A_{600}$ ) following the shift from galactose to glucose. *C*, the relative ratio of HA-tagged *eIF4E* and HA-tagged *eIF2A* as determined densitometrically from *A*. *D*, time course of HA-tagged *eIF4E* and HA-tagged *eIF2A* degradation in *eIF2A* $\Delta$  yeast cells. The quantitative data from *C* are plotted as log (relative intensity) versus time in order to estimate the protein half-life of HA-tagged *eIF4E* and HA-tagged *eIF2A*. Under the experimental conditions, no loss of HA-tagged *eIF4E* was observed, whereas HA-tagged *eIF2A* disappeared with a half-life of 17–18 min. *E*, Northern blot analysis of mRNA for HA-tagged *eIF2A* and HA-tagged *eIF4E* expressed in the *eIF2A* $\Delta$  strain. Total RNA was isolated from *eIF2A* $\Delta$  yeast strain harboring plasmids expressing HA-tagged *eIF2A* and HA-tagged *eIF4E* at 0, 10, 20, and 30 min following the switch from galactose to glucose. For each lane, 15  $\mu$ g of total yeast RNA was separated on a denaturing agarose gel, transferred onto BrightStart-Plus nylon membrane (Ambion), and hybridized to a  $^{32}$ P-labeled DNA HA probes. The half-life of both mRNAs was less than 10 min. *F*, Western blot analysis of the *eIF2A* $\Delta$  strain transformed with an HA-tagged *eIF2A* clones. Custom made antibodies derived against a central core fragment (Gly<sup>59</sup>–Glu<sup>420</sup>) of recombinant *eIF2A* were used. Samples were prepared as in *A*. Protein loading control is shown to the right of the Western blot.

(57, 58). Remarkably most of these IRES elements initiate translation of proteins that protect cells from stress or at least help them to cope with transient stress conditions (57, 58). The exact molecular mechanisms that redirect the ribosome from

the m<sup>7</sup>G cap structure to the IRES elements under such conditions are unknown. One simple possibility is that the inhibition of cap-dependent translation through sequestration of *eIF4E* by the *eIF4E* binding protein frees other initiation fac-

tors for the IRES-mediated processes. Few of the IRES-containing mRNAs require the cap-binding factor eIF4E or intact eIF4G (*i.e.* missing the eIF4E-binding domain in the N terminus) for their translation (57) and, under conditions of reduced global translation, mRNAs containing IRES elements generally become more competitive for ribosome binding.

We have also shown here that eIF2A functions as a suppressor of IRES-mediated translation in yeast *S. cerevisiae* at least as tested using the Ure2p IRES reporter system. The mechanistic basis for this increased induction of Ure2p IRES expression in *eIF2AΔ* cells over what is seen in the WT yeast is unclear. Two possibilities exist. First, eIF2A might act directly by slowing the rate of IRES-containing mRNA binding to 40 S subunits or by slowing the steps between the 48 S complex and the elongating 80 S ribosome. In this regard, the finding of eIF2A bound to 40 and 80 S ribosomes would support this suggestion (14). Second, eIF2A might function indirectly by affecting the synthesis of some protein that directly influences IRES-mediated expression. Given that mammalian eIF2A was previously shown to not stimulate expression from globin mRNA (7), it is possible that eIF2A specifically binds and affects the translation of only a subset of mRNAs such as IRES-containing mRNAs. If one assumes a mechanism for eIF2A function based upon its similarity in biochemical properties to those of IF2 (binding of an aminoacyl-tRNA to ribosomes in a codon-dependent manner), it would appear likely that eIF2A actively participates in the initiation process. The finding of eIF2A in 48 and 80 S complexes (Fig. 4 and data in Ref. 14), and the fact that it marginally affects cap-dependent initiation supports this suggestion. We hypothesize that the release of eIF2A from 48 and 80 S complexes is much slower than the release of eIF2, and thus, although eIF2A is functioning in a positive, synthetic direction, the fact that it is acting so much more slowly than eIF2 results in "apparent suppression," causing a delay in the transition of the 80 S ribosome to the elongation cycle. This suggestion is supported by an earlier observation on AUG-directed methionyl-puromycin synthesis using salt-washed ribosomes and purified rabbit eIF2 and eIF2A (7).

Consistent with this hypothesis is the observation in yeast that human eIF2A can only partially suppress Ure2p IRES activity and was found to be less abundant in the 80 S ribosomes (Fig. 4B). At the same time, no change in *URE2* IRES activity was observed in *eIF5BΔ* cells, and the binding of the yeast eIF2A to 40 and 80 S ribosomes was not impaired either. The accumulation of eIF2A in 80 S complexes in *prt1-1* cells at the nonpermissive temperature also supports the suggestion that eIF2A might act during the transition of the 80 S initiation complex to the elongating 80 S ribosome (eIF2A is assumed to be released during this transition, since it is not found in polysomes (14)).

Taking together the genetic and biochemical data and assuming the nature of eIF2A being a translation initiation factor, one might suggest that eIF2A is involved in a process that impinges on the expression of many specific proteins. The expression of these proteins in yeast can be controlled by IRES elements. Since the deletion of eIF2A in the *eIF4E-ts* background results in slow growth and altered phenotype, we anticipate that several IRES-containing mRNAs are up-regulated and either directly or indirectly lead to the aberrant phenotypes we have observed. Although only proven for the Ure2p IRES element, we hypothesize that eIF2A might act as a global suppressor of IRES-mediated expression allowing for translational control through the levels of eIF2A protein, since eIF2A was found to be an inherently unstable protein. Future experiments are required to determine if this is indeed the case.

**Acknowledgments**—We thank Dr. Nahum Sonenberg for providing the pDAD2-eIF4E(HA tag) plasmid and Dr. Biao Li for pMW127 plasmid. Dr. Thomas Dever is kindly acknowledged for providing the GIM3Δ, GIM5Δ, PAC10Δ, PRT1, and the *prt1-1* yeast strains. We also thank Drs. Thomas Dever, Maria Hatzoglou, and C. Ramana Bhaskar for helpful discussions during the course of this work and Drs. Hans Trachsel and Michael Altmann for critical reading of the manuscript. Flow cytometry was performed in the CINJ/NIEHS Analytical Cytometry Image Analysis Core Facility, and fluorescent microscopy was performed in the Robert Wood Johnson Medical School Department of Pharmacology.

## REFERENCES

- Hershey, J. W. B., and Merrick, W. C. (2000) in *Translational Control of Gene Expression* (Sonenberg, N., Hershey, J. W. B., and Mathews, M. B., eds) pp. 33–38, Cold Spring Harbor Laboratory Press, Cold Spring Harbor, NY
- Sonenberg, N., and Dever, T. E. (2003) *Curr. Opin. Struct. Biol.* **13**, 56–63
- Mathews, M. B., Sonenberg, N., and Hershey, J. W. B. (2000) in *Translational Control of Gene Expression* (Sonenberg, N., Hershey, J. W. B., and Mathews, M. B., eds) pp. 1–31, Cold Spring Harbor Laboratory Press, Cold Spring Harbor, NY
- Gingras, A. C., Raught, B., and Sonenberg, N. (2001) *Genes Dev.* **15**, 807–826
- Dever, T. E. (2002) *Cell* **108**, 545–556
- Merrick, W. C., and Anderson, W. F. (1975) *J. Biol. Chem.* **250**, 1197–1206
- Adams, S. L., Safer, B., Anderson, W. F., and Merrick, W. C. (1975) *J. Biol. Chem.* **250**, 9083–9089
- Benne, R., Brown-Luedi, M. L., and Hershey, J. W. B. (1979) *Methods Enzymol.* **60**, 15–35
- Majumdar, A., Dasgupta, A., Chatterjee, B., Das, K. H., and Gupta, N. K. (1979) *Methods Enzymol.* **60**, 35–52
- Staehelein, T., Erni, B., and Schreier, M. H. (1979) *Methods Enzymol.* **60**, 136–165
- Gupta, N. K., Woodley, C. L., Chen, Y. C., and Bose, K. K. (1973) *J. Biol. Chem.* **248**, 4500–4511
- Levin, D. H., Kyner, D., and Acs, G. (1973) *Proc. Natl. Acad. Sci. U. S. A.* **70**, 41–45
- Merrick, W. C., Kemper, W. M., and Anderson, W. F. (1975) *J. Biol. Chem.* **250**, 5556–5562
- Zoll, W. L., Horton, L. E., Komar, A. A., Hensold, J. O., and Merrick, W. C. (2002) *J. Biol. Chem.* **277**, 37079–37087
- Altmann, M., Sonenberg, N., and Trachsel, H. (1989) *Mol. Cell. Biol.* **10**, 4467–4472
- Altmann, M., and Trachsel, H. (1997) *Methods* **11**, 343–352
- Rose, M. D., Winston, F., and Heiter, P. (1990) *Methods in Yeast Genetics: A Laboratory Course Manual*, Cold Spring Harbor Laboratory, Cold Spring Harbor, NY
- Ito, H., Fukuda, Y., Murata, K., and Kimura, A. (1983) *J. Bacteriol.* **53**, 163–168
- Mueller, P. P., Harashima, S., and Hinnebusch, A. G. (1987) *Proc. Natl. Acad. Sci. U. S. A.* **84**, 2863–2867
- Komar, A. A., Lesnik, T., Cullin, C., Merrick, W. C., Trachsel, H., and Altmann, M. (2003) *EMBO J.* **22**, 1199–1209
- Alwine, J. C., Kemp, D. J., and Stark, G. R. (1977) *Proc. Natl. Acad. Sci. U. S. A.* **74**, 5350–5354
- Towbin, H., Staehelin, T., and Gordon, J. (1979) *Proc. Natl. Acad. Sci. U. S. A.* **76**, 4350–4354
- Hinck, A. P., Walkenhorst, W. F., Westler, W. M., Choe, S., and Markley, J. L. (1993) *Protein Eng.* **6**, 221–227
- Ukiyama, E., Jancso-Radek, A., Li, B., Milos, L., Zhang, W., Phillips, N. B., Morikawa, N., King, C. Y., Chan, G., Haqq, C. M., Radek, J. T., Poulat, F., Donahoe, P. K., and Weiss, M. A. (2001) *Mol. Endocrinol.* **15**, 363–377
- Sambrook, J., Fritsch, F. F., and Maniatis, T. (1989) *Molecular Cloning: A Laboratory Manual*, 2nd Ed., Cold Spring Harbor Laboratory, Cold Spring Harbor, NY
- Laemmli, U. K. (1970) *Nature* **227**, 680–685
- Schagger, H., and von Jagow, G. (1987) *Anal. Biochem.* **166**, 368–379
- Entian, K. D., Schuster, T., Hegemann, J. H., Becher, D., Feldmann, H., Guldener, U., Gotz, R., Hansen, M., Hollenberg, C. P., Jansen, G., Kramer, W., Klein, S., Kotter, P., Kricke, J., Launhardt, H., Mannhaupt, G., Maierl, A., Meyer, P., Mewes, W., Munder, T., Niedenthal, R. K., Ramezani Rad, M., Rohmer, A., Romer, A., Rose, M., Schafer, B., Sieglar, M. L., Vetter, J., Wilhelm, N., Wolf, K., Zimmermann, F. K., Zollner, A., and Hinne, A. (1999) *Mol. Gen. Genet.* **262**, 683–702
- Winzler, E. A., Shoemaker, D. D., Astromoff, A., Liang, H., Anderson, K., Andre, B., Bangham, R., Benito, R., Boeke, J. D., Bussey, H., Chu, A. M., Connelly, C., Davis, K., Dietrich, F., Dow, S. W., El Bakkoury, M., Foury, F., Friend, S. H., Gentalen, E., Giaever, G., Hegemann, J. H., Jones, T., Laub, M., Liao, H., Liebundguth, N., Lockhart, D. J., Lucau-Danila, A., Lussier, M., MRabet, N., Menard, P., Mittmann, M., Pai, C., Rebischung, C., Revuelta, J. L., Riles, L., Roberts, C. J., Ross-MacDonald, P., Scherens, B., Snyder, M., Sookhai-Mahadeo, S., Storms, R. K., Veronneau, S., Voet, M., Volckaert, G., Ward, T. R., Wysocki, R., Yen, G. S., Yu, K., Zimmermann, K., Philippsen, P., Johnston, M., and Davis, R. W. (1999) *Science* **285**, 901–906
- Brenner, C., Nakayama, N., Goebel, M., Tanaka, K., Toh-e, A., and Matsumoto, K. (1988) *Mol. Cell. Biol.* **8**, 3556–3559
- Danaie, P., Altmann, M., Hall, M. N., Trachsel, H., and Helliwell, S. B. (1999) *Biochem. J.* **340**, 135–141
- Drubin, D. G. (2000) *Cell Polarity*, Oxford University Press, Oxford, UK
- Saito, T. L., Ohtani, M., Sawai, H., Sano, F., Saka, A., Watanabe, D., Yukawa, M., Ohya, Y., Morishita, S. (2004) *Nucleic Acids Res.* **32**, 319–322
- Madden, K., and Snyder, M. (1998) *Annu. Rev. Microbiol.* **52**, 687–744

35. Karpova, T. S., McNally, J. G., Moltz, S. L., and Cooper, J. A. (1998) *J. Cell Biol.* **142**, 1501–1517
36. Altmann, M., Muller, P. P., Wittmer, B., Ruchti, F., Lanker, S., and Trachsel, H. (1993) *EMBO J.* **12**, 3997–4003
37. Tong, A. H., Lesage, G., Bader, G. D., Ding, H., Xu, H., Xin, X., Young, J., Berriz, G. F., Brost, R. L., Chang, M., Chen, Y., Cheng, X., Chua, G., Friesen, H., Goldberg, D. S., Haynes, J., Humphries, C., He, G., Hussein, S., Ke, L., Krogan, N., Li, Z., Levinson, J. N., Lu, H., Menard, P., Munyana, C., Parsons, A. B., Ryan, O., Tonikian, R., Roberts, T., Sdicu, A. M., Shapiro, J., Sheikh, B., Suter, B., Wong, S. L., Zhang L. V., Zhu, H., Burd, C. G., Munro, S., Sander, C., Rine, J., Greenblatt, J., Peter, M., Bretscher, A., Bell, G., Roth, F. P., Brown, G. W., Andrews, B., Bussey, H., and Boone, C. (2004) *Science* **303**, 808–813
38. Nielsen, K. H., Szamecz, B., Valasek, L., Jivotovskaya, A., Shin, B. S., and Hinnebusch, A. G. (2004) *EMBO J.* **23**, 1166–1177
39. Schneider, B. L., Patton, E. E., Lanker, S., Mendenhall, M. D., Wittenberg, C., Futcher, B., and Tyers, M. (1998) *Nature* **395**, 86–89
40. Johnston, M., Flick, J. S., and Pexton, T. (1994) *Mol. Cell. Biol.* **6**, 3834–3841
41. Rogers, S. W., Wells, R., and Rechsteiner, M. (1986) *Science* **234**, 364–368
42. Rechsteiner, M., and Rogers, S. W. (1996) *Trends Biochem. Sci.* **21**, 267–271
43. Peng, J., Schwartz, D., Elias, J. E., Thoreen, C. C., Cheng, D., Marsischky, G., Roelofs, J., Finley, D., and Gygi, S. P. (2003) *Nat. Biotechnol.* **21**, 921–926
44. Varshavsky, A. (1996) *Proc. Natl. Acad. Sci.* **93**, 12142–12149
45. Vainberg, I. E., Lewis, S. A., Rommelaere, H., Ampe, C., Vandekerckhove, J., Klein, H. L., and Cowan, N. J. (1998) *Cell* **93**, 863–873
46. Hansen, W. J., Cowan, N. J., and Welch, W. J. (1999) *J. Cell Biol.* **145**, 265–277
47. Cooper, J. A., and Schafer, D. A. (2000) *Curr. Opin. Cell Biol.* **12**, 97–103
48. Liu, H., Krizek, J., and Bretscher, A. (1992) *Genetics* **132**, 665–673
49. Norden, C., Liakopoulos, D., and Barral, Y. (2004) *Mol. Microbiol.* **53**, 469–483
50. Pyronnet, S., and Sonenberg, N. (2001) *Curr. Opin. Genet. Dev.* **11**, 13–18
51. Kimball, S. R. (1999) *Int. J. Biochem. Cell Biol.* **31**, 25–29
52. Clemens, M. J. (2001) *Prog. Mol. Subcell. Biol.* **27**, 57–89
53. Clemens, M. J. (2001) *J. Cell Mol. Med.* **5**, 221–239
54. Proud, C. G. (2001) *Prog. Mol. Subcell. Biol.* **26**, 95–114
55. Prevot, D., Darlix, J. L., and Ohlmann, T. (2003) *Biol. Cell* **95**, 141–156
56. Johannes, G., Carter, M. S., Eisen, M. B., Brown, P. O., and Sarnow, P. (1999) *Proc. Natl. Acad. Sci. U. S. A.* **96**, 13118–13123
57. Hellen, C. U., and Sarnow, P. (2001) *Genes Dev.* **15**, 1593–1612
58. Bonnal, S., Boutonnet, C., Prado-Lourenco, L., and Vagner, S. (2003) *Nucleic Acids Res.* **31**, 427–428
59. Clontech (2001) *Yeast Protocols Handbook*, Clontech, Palo Alto, CA



**Novel Characteristics of the Biological Properties of the Yeast *Saccharomyces cerevisiae* Eukaryotic Initiation Factor 2A**

Anton A. Komar, Stephane R. Gross, Diane Barth-Baus, Ryan Strachan, Jack O. Hensold,  
Terri Goss Kinzy and William C. Merrick

*J. Biol. Chem.* 2005, 280:15601-15611.

doi: 10.1074/jbc.M413728200 originally published online February 16, 2005

---

Access the most updated version of this article at doi: [10.1074/jbc.M413728200](https://doi.org/10.1074/jbc.M413728200)

Alerts:

- [When this article is cited](#)
- [When a correction for this article is posted](#)

[Click here](#) to choose from all of JBC's e-mail alerts

This article cites 53 references, 23 of which can be accessed free at <http://www.jbc.org/content/280/16/15601.full.html#ref-list-1>